Dual-frequency liquid crystals as tunable materials for beam steering in terahertz photonics

Oleksandra Gridyakina[1*], Urszula Chodorow[2], Adrianna Nieradka[1], Agnieszka Siemion[1], Janusz Parka[2], Piotr Lesiak[1] and Tomasz R. Woliński[1]

[1] *Warsaw University of Technology, Faculty of Physics, Koszykowa 75, 00-662 Warsaw, Poland*
[2]*Military University of Technology, Faculty of Advanced Technologies and Chemistry, Kaliskiego 2, 00-908 Warsaw, Poland*

Received October 24, 2025; accepted December 30, 2025; published December 31, 2025

Abstract—Dual-frequency liquid crystal (LC) materials for tunable beam steering in the 0.1–3.5 THz range were investigated. Recent LC formulations exhibit a low loss tangent, high polarization coefficients, and significant dielectric and optical anisotropies, including suitably high birefringence for effective THz modulation. We have implemented this material in electrically tunable phase shifters and beam-steering elements, demonstrating their ability to operate with low absorption and controllable birefringence. The obtained characteristics suggest that dual-frequency LCs could be used to create compact, efficient, and highly tunable THz photonic and sensing components. This study outlines the performance parameters relevant to practical THz devices and highlights their potential for reconfigurable photonic architectures.

Terahertz (THz) radiation, typically defined in the 0.1–10 THz range, has attracted growing scientific and technological interest. This part of the electromagnetic spectrum remains one of the least explored, yet it offers unique advantages for sensing, imaging, spectroscopy, and communications. THz waves are strongly attenuated in conductive materials but propagate well through many dielectrics. Due to their low photon energy, they do not ionize matter, making them promising for material inspection and safe, non-destructive testing applications [1].

The development of compact THz systems requires high-performance devices that can efficiently control and modulate THz beams. Conventional THz optical components often suffer from low birefringence, high losses, and limited tunability [2]. Metasurface-based solutions offer improved flexibility but are limited by dispersion and fabrication complexity, and most are non-reconfigurable after fabrication [3, 4]. In contrast, liquid crystals (LCs) offer large optical anisotropy and can be tuned thermally or electrically, making them attractive for manipulating THz beams [5, 6].

However, pure nematic LCs usually exhibit lower birefringence in the THz range than in the visible region, which reduces their effectiveness [7, 8]. LC mixtures designed for the THz domain often provide better performance, but their properties remain strongly dependent on molecular structure and composition [9–12]. Even small chemical modifications may significantly change absorption, refractive index, and birefringence. For this reason, systematic studies of structure–property relationships are essential for designing LCs suitable for THz applications.

One of the main limitations is the long relaxation time required for thick LC layers to achieve THz phase control. For an LC cell operating in the THz region (λ = 0.03–3 mm), a thicker cell gap is required in order to achieve the same phase change $\delta = 2\pi d\Delta n/\lambda$, where d is the LC cell gap, Δn is the LC birefringence, and λ is the wavelength. Also, it is well known that as the wavelength increases, Δn decreases and then gradually saturates [13]. Thus, a relatively large cell gap is required for operation in the THz region, which results in a slow response time. Consequently, as the LC layer thickness increases, the response time also increases as d^x, where $x = 2$ for the case of strong anchoring and $x \to 1$ when the anchoring is weak [14, 15]. Dual-frequency liquid crystals (DFLCs) offer a promising solution because their dielectric anisotropy changes sign with the frequency of the applied voltage [16, 17]. This property enables faster ON–OFF switching by driving the LC with high-frequency electrical pulses.

Beam steering is a key function in many optical and photonic systems, including LiDAR, telecommunications, microscopy, and sensing. Mechanical steering approaches offer high precision but suffer from limited lifetime, slow response, and high power consumption [18]. Non-mechanical methods, particularly LC-based solutions, provide lightweight, low-power, and compact alternatives [19]. Despite significant progress in the visible and near-infrared regions, efficient LC-based beam steering in the THz domain is still challenging due to slow response times and high operating voltages. This work aims to investigate the potential of dual-frequency LC materials for tunable THz beam steering. Special attention is given to the relationship between molecular structure, birefringence, absorption, and polarization properties in the 0.1–3 THz region. The results offer insight into material optimization

* e-mail: oleksandra.gridyakina@pw.edu.pl

strategies and support the development of compact, reconfigurable terahertz (THz) photonic components.

The measurements of DFLC optical properties were performed using a THz time domain spectroscopy (THz-TDS) - the TeraView TeraPulse Lx Modular System at room temperature. To eliminate the adverse effects of atmospheric water vapor, the sample was placed in a dry air chamber during THz-TDS transmission measurements [20]. Moreover, to reduce unwanted reflection effects and ensure more reliable measurement results, a Blackman-Harris 4-term (BH4) anodization filter was applied when analyzing the data. The LC cells were assembled from two z-cut quartz plates, each 1.5mm thick, with a 500µm DFLC layer sandwiched between them. Copper wires served simultaneously as separators and electrodes. Two cell configurations were used: HT, which provides homeotropic alignment of the DFLC, and HG, ensuring homogeneous (planar) alignment without the application of voltage. The reference signal was obtained using two directly adjacent quartz plates, each 1.5 mm thick. In our experiments, a rectangular waveform of 400 V was applied across the LC cell electrodes (spacing ~13 mm, ≈ 30 V/mm). At 100 Hz, the director adopted a planar state, whereas at 100 kHz, it switched to a homeotropic orientation (Fig. 1). The inset in Fig. 1 shows a view of the molecules inside the cell, as observed along the voltage applied to the electrodes at a frequency of 100 kHz. The long axes of the molecules are aligned perpendicularly to the applied voltage, but around this direction, they are free to arrange themselves.

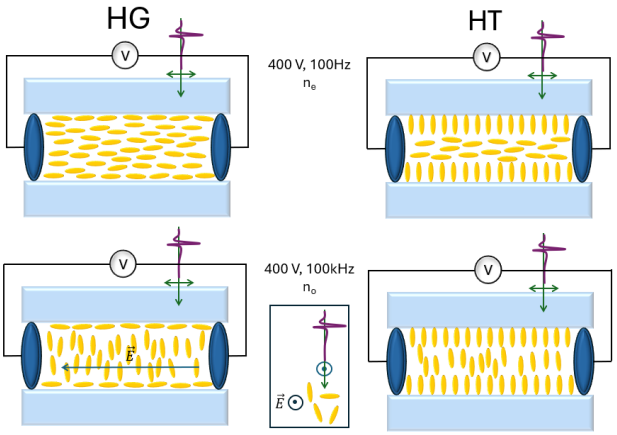

Fig. 1. Schematic configurations of the HT and HG cells used in the experiment. The application of a dual-frequency driving field (100 Hz/100 kHz) enables switching between the n_e and n_o states in both geometries.

The time-domain pulse signals of the reference $E_r(t)$ and the sample $E_s(t)$ can be measured by a THz-TDS system. The result of measurement is an electro-optical signal versus time (Fig. 2). After the Fourier transform, their amplitudes $E_r(\omega)$, $E_s(\omega)$, and phases $\delta_r(\omega)$, $\delta_s(\omega)$ of the reference and samples in the frequency domain are obtained, correspondingly. The transmission amplitude is $A(\omega)=E_s(\omega)/E_r(\omega)$ and the phase shift between the sample and the reference is $\Delta\delta=\delta_s(\omega)-\delta_r(\omega)$. Therefore, the effective refractive index $n(\omega)$ and absorption coefficient $\alpha(\omega)$ can be calculated by [12]:

$$n(\omega)=1+\frac{c\Delta\delta(\omega)}{\omega d} \text{ and } \alpha(\omega)=-\frac{2}{d}\cdot\ln\left(\frac{A(\omega)\left[n(\omega)+1\right]^2}{4n(\omega)}\right),$$

where c is the speed of light in vacuum, ω is the angular frequency, and d is the thickness of the samples.

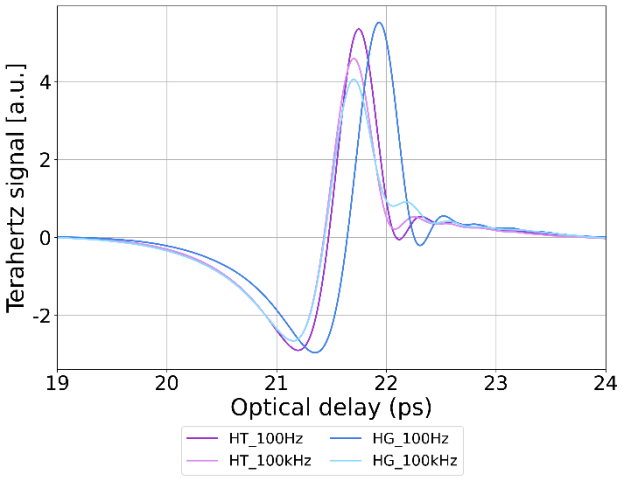

Fig. 2. The result of TDS measurement (an electro-optical signal versus time -THz waveform transmitted through reference and sample cell) for ordinary and extraordinary beams in HT and HG cells.

The coefficients for ordinary and extraordinary rays were obtained by using the same equations as above. The ordinary coefficients were measured when the polarization of a THz wave was perpendicular to an LC director. When the polarization of an incident THz wave was parallel to an LC director, extraordinary indices were obtained. For clarity, in this work we refer to the field-induced ordinary-like and extraordinary-like orientations as the n_o-state and n_e-state, respectively.

A dual-frequency, multi-component mixture 1859 (Military University of Technology, Warsaw, Poland) [21] was investigated. The material exhibits positive dielectric anisotropy at low driving frequencies and negative anisotropy at high frequencies, enabling frequency-controlled reorientation. The crossover frequency lies in the tens of kilohertz range and shifts with temperature. The mixture contains fluorinated and isothiocyanate-substituted components, exhibiting a broad nematic range from approximately –20°C to 70°C.

The refractive index spectra obtained for the HG and HT cells (Fig. 3) clearly reveal the dependence of the measured indices on the initial director configuration and the applied dual-frequency driving conditions. At 0 V, the initial alignment determines the detected refractive index: the HG cell exhibits the extraordinary index n_e, while the HT cell provides the ordinary index n_o. Upon applying a 400 V

driving field, the switching behavior follows the expected dual-frequency response. In the high-frequency regime (100 kHz), both cell types reorient toward the ordinary index, yielding approximate values of $n_o \approx 1.48$–1.52 for HG and $n_o \approx 1.53$–1.58 for HT in the studied THz range. Under low-frequency excitation (100 Hz), the director aligns along the extraordinary axis, resulting in $n_e \approx 1.64$–1.65 for HG and $n_e \approx 1.60$–1.63 for HT.

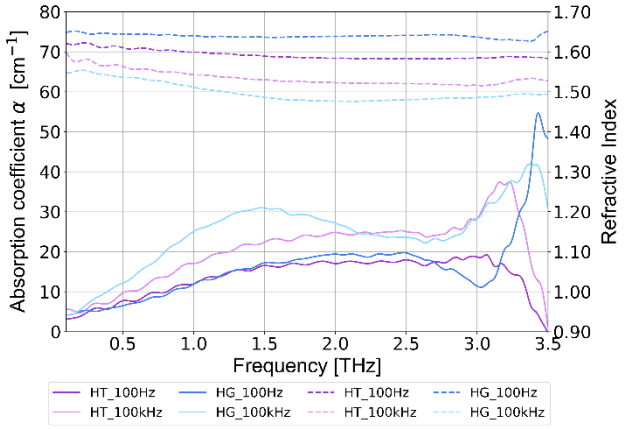

Fig. 3. Refractive indices (dashed) and absorbance (solid) versus frequency for n_o and n_e in HT and HG cells.

As shown in Fig. 3, the HG cell exhibits a significantly larger birefringence $\Delta n = n_e - n_o$, with values of approximately 0.10–0.17 across the THz range, whereas the HT cell consistently demonstrates a smaller value $\Delta n \approx 0.04$–0.07. Both n_e and n_o follow characteristic dispersion trends of the DFLC 1859 mixture: the extraordinary index (e.g., HG at 400 V, 100 Hz) increases with frequency above ~1.5 THz, while the ordinary index (at 0 V or 400 V, 100 kHz) decreases with frequency, reaching its minimum near 2.0 THz. A comparison of the two configurations reveals that the HG cell offers a broader birefringence window, stronger anisotropy, and more effective switching, whereas the HT cell exhibits notably slower switching and reduced tunability. The reduced performance of the HT configuration suggests a less complete reorientation of the liquid crystal director—likely due to stronger anchoring or alignment constraints—resulting in a narrower and less responsive tuning range.

The absorption characteristics of the HG and HT cells (Fig. 3) show clear differences in their optical behavior. In the HG cell, the absorption coefficient α depends strongly on the director orientation. The n_o-state (0 V) has much higher absorption than the n_e-state (400 V, 100 Hz), with the largest difference appearing near 2.0 THz. This indicates a strong absorption anisotropy in the planar-aligned cell. In contrast, the HT cell shows absorption curves that lie very close to each other for all applied voltages in the THz range studied. The small separation between α_e and α_o confirms that the HT cell provides only weak anisotropy and limited tuning of the absorption compared to the HG configuration.

The results show that the DFLC 1859 mixture enables effective and reversible tuning of its THz optical properties under an external electric field. The HG (planar) cell exhibits a significantly stronger electro-optical response, including larger birefringence, higher refractive index contrast, and clearer absorption differences, confirming efficient switching between the low-frequency (n_e) and high-frequency (n_o) states. The HT (homeotropic) cell shows weaker reorientation, smaller anisotropy, and reduced changes in both refractive index and absorption, likely due to stronger vertical anchoring. Overall, planar alignment provides better field-induced tunability in the THz range. Future work will examine gold-nanoparticle-doped LCs to improve switching speed and reduce the required voltage.

This work was funded by the National Science Centre, Poland, UMO-2023/05/Y/ST11/00238 M-ERA.NET 3 project and supported by the Excellence Initiative Research University of the Warsaw University of Technology.

References

[1] M. Mittendorff, S. Li, T.E. Murphy, ACS Photonics **4**, 316 (2017).
[2] K. Wiesauer, C. Jördens, J. Infrared Milli Terahz Waves **34**, 663 (2013).
[3] L. Zhang, S. Mei, K. Huang, C.-W. Qiu, Adv. Opt. Materials **4**, 818 (2016).
[4] W.L. Chan, H.-T. Chen, A.J. Taylor, I. Brener, M.J. Cich, D.M. Mittleman, Appl. Phys. Lett. **94**, 213511 (2009).
[5] L. Yang, F. Fan, M. Chen, X. Zhang, J. Bai, S. Chang, Opt. Mater. Expr. **6**, 2803 (2016).
[6] L. Cattaneo, M. Savoini, I. Muševič, A. Kimel, T. Rasing, Opt. Expr. **23**, 14010 (2015).
[7] R. Wilk, N. Vieweg, O. Kopschinski, T. Hasek, M. Koch, J. Infrared Milli Terahz Waves **30**, 1139 (2009).
[8] N. Vieweg, C. Jansen, M.K. Shakfa, M. Scheller, N. Krumbholz, R. Wilk, M. Mikulics, M. Koch, Opt. Expr. **18**, 6097 (2010).
[9] C. Weil, St. Müller, P. Scheele, P. Best, G. Lüssem, R. Jakoby, Electron. Lett. **39**, 1732 (2003).
[10] L. Wang, X. Lin, X. Liang, J. Wu, W. Hu, Z. Zheng, B. Jin, Y. Qin, Y. Lu, Opt. Mater. Expr. **2**, 1314 (2012).
[11] U. Chodorow, J. Parka, K. Garbat, N. Pałka, K. Czupryński, Phase Transitions **85**, 337 (2012).
[12] U. Chodorow, J. Parka, O. Chojnowska, Photon. Lett. Poland **4**, 112 (2012).
[13] S.-T. Wu, Phys. Rev. A **33**, 1270 (1986).
[14] E. Jakeman, E. P. Raynes, Phys. Lett. A **39**, 69 (1972).
[15] X. Nie, R. Lu, H. Xianyu, T.X. Wu, S.-T. Wu, J. Appl. Phys. **101**, 103110 (2007).
[16] H.K. Bücher, R.T. Klingbiel, J.P. VanMeter, Appl. Phys. Lett. **25**, 186 (1974).
[17] H. Xianyu, S.-T. Wu, C.-L. Lin, Liquid Crystals **36**, 717 (2009).
[18] R.E. Fischer, B. Tadic-Galeb, P.R. Yoder, Optical System Design (McGraw-Hill, 2008).
[19] Z. He, F. Gou, R. Chen, K. Yin, T. Zhan, S.-T. Wu, Crystals **9**, 292 (2019).
[20] D.M. Slocum, E.J. Slingerland, R.H. Giles, T.M. Goyette, J. Quant. Spectrosc. Radiat. Transfer **127**, 49 (2013).
[21] P. Perkowski, M. Mrukiewicz, M. Laska, K. Garbat, W. Piecek, R. Dąbrowski, Phase Transit. **86**, 113 (2013).